

콘크리트의 구속효과와 재료비선형을 고려한 내부 구속 CFT 기둥의 축력-모멘트 상호작용 분석

Analysis of the Axial Force-Bending Moment Interaction for a CFT Column Considering the Confining Effect and the Material Nonlinearity of Concrete

한택희* · 염응준** · 윤기용*** · 이창수**** · 강진욱***** · 강영종*****

Han, Taek-Hee · Youm, Eung-Jun · Yoon, Ki-Yong · Lee, Chang-Soo · Kang, Jin-Ook · Kang, Young-Jong

ABSTRACT

Concrete in a CFT(Concrete Filled Tube) column has enhanced strength and ductility because it is triaxially confined by a steel tube. But CFT columns are designed based on linear analyses by stress block method without the confining effect or the nonlinearity of the concrete. These make the significantly difference between the analysis results and the experimental results. Thus in this study, a nonlinear CFT column model was developed considering the confining effect on the concrete in a CFT column. This developed model was verified by experimental results from other researchers and compared with the results of various specifications. With the developed model, parametric studies were performed and the developed column model showed reasonable and accurate results.

Keywords : CFT, column, nonlinear, confined concrete, interaction

1. Introduction

A steel tube offer continuous confining pressure on the concrete in a CFT column. Thus the strength of confined concrete by a steel tube is much larger than that of unconfined plain concrete. This fact means the increased strength of the confined concrete should be considered when a CFT column is analyzed. But recommended methods to plot interaction diagrams of CFT columns by current specifications like AISC-LRFD, AIJ-ASD, and CAN/CSA are not considering this confining effect because of the reason that it is difficult to compute the realistic stress of the confined concrete. In these

* 정희원 · 고려대학교 공학기술연구소 연구조교수 · 공학박사 E-mail: taekie@korea.ac.kr

** 고려대학교 사회환경시스템공학과 박사과정 · 공학석사 E-mail: trussbassist@hanmail.net

*** 정희원 · 충남대학교 토목공학과 조교수 · 공학박사 E-mail: kyyoon@sunmoon.ac.kr

**** 삼성물산(주) 건설부문 토목기술팀 부장 · 공학사 E-mail: ms2ce@samsung.com

***** 삼성물산(주) 건설부문 토목기술팀 차장 · 공학박사 E-mail: jin.kang@samsung.com

***** 정희원 · 고려대학교 사회환경시스템공학과 교수 · 공학박사 E-mail: yjkange@korea.ac.kr

specifications, forces and moments are calculated from assumed stress block and these methods cannot consider the material nonlinearities and the increase of the confined concrete. The generally used calculation process is illustrated in Fig. 1 for one particular strain distribution. The cross section and one assumed strain distribution are shown in Fig. 1. The maximum compressive strain (ϵ_{cu}) is set 0.0035, corresponding to failure of the section. The location of the neutral axis and the strain in each level of reinforcement are computed from the strain distribution.

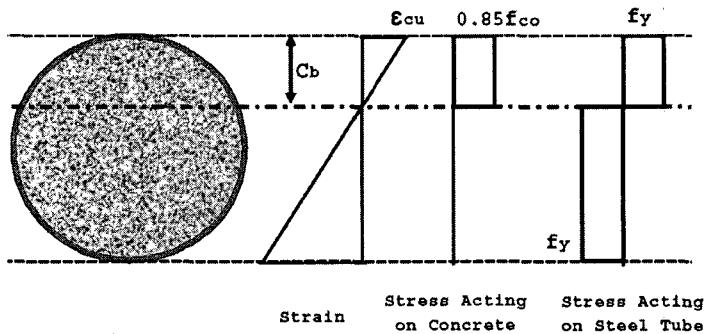


Fig. 1 Calculation of Axial Force and Moment by Current Specifications

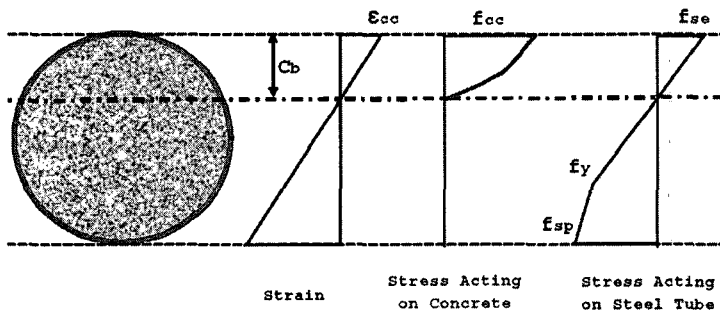


Fig. 2 Calculation of Axial Force and Moment by Proposed Method

2. Proposed Nonlinear Method

According to the methods guided by current specifications, the compressive force on the concrete is computed from the assumed stress block. The stress block is assumed to have the magnitude of 85% of the unconfined concrete strength (f_{co}) and the distributed length of the stress block is assumed to be 85% of the distance between the neutral axis and the outer surface of the column (C_b). And the forces on the steel tube are computed from the assumed stress block which has the quantity of yield stress (f_{STy}). The axial force (P_n) is computed by summing the individual forces in concrete and steel, and the moment (M_n) is computed by summing the moments of these forces about the geometric centroid of the cross section. These values of P_n and M_n represent one point on the interaction diagram. But this method is too conservative and inaccurate because it doesn't consider the increase of the concrete

strength confined by a steel tube. Fam, Qie and Rizkalla (2004) showed that the interaction results of CFT columns calculated from the specifications are significantly different from the realistic behavior of a CFT column by their experimental researches. Thus, a new method is necessary to plot interaction diagrams considering the confining effect by the steel tube and material nonlinearities of concrete and steel. In this method, the corresponding stresses in each layer of the concrete are computed from the developed concrete models in previous chapter with considering the increased strength of the confined concrete. The calculation process is illustrated in Fig. 2 for one particular strain distribution.

The maximum compressive strain (ϵ_{cou}) on the outer surface of the column depends on the maximum compressive strain (ϵ_{cc}) of the confined concrete and it is computed from the developed concrete model. This maximum compressive of the confined concrete is located at the contacting surface of the concrete and the steel tube. The stress in the concrete is computed corresponding strain from the developed concrete models. And the forces in the concrete are computed by integrating the stresses in each layer. And also the moments in the concrete are computed by the integrating the product of the force and the distance from the centroid at each layer. The force and moment in steel are calculated by the same process. The material model of the steel is assumed a bilinear model. If the stress corresponding the strain at a certain point is larger than yield stress, it is computed considering the strain hardening of steel. If strain of steel exceeds its ultimate strain, corresponding stress in steel is zero and the steel tube is assumed to be ruptured. The total axial force and moment are calculated by summing the individual forces and moments in concrete and steel. The used material models are shown in Fig. 8 and Fig. 9.

2.1 Derivation of Computation Method

To plot interaction diagrams, it is necessary to compute the various interaction points by using strain compatibility and mechanics. Axial force and moment in each part of the column section are calculated and the total axial force (P_n) and total moment (M_n) are computed by summing their each component for every step which the strain distribution changes. For this calculation, bilinear models and nonlinear models are adopted as steel and concrete models respectively. And also a computer program is developed to plot interaction diagrams considering the confining effect or not.

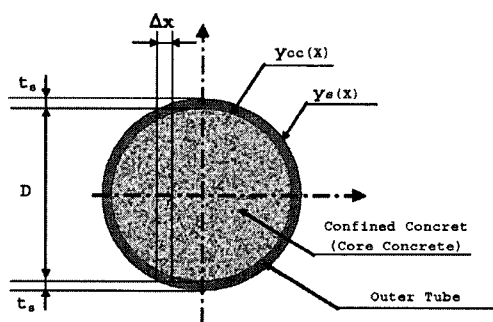


Fig. 3 Cross Section of a CFT Column

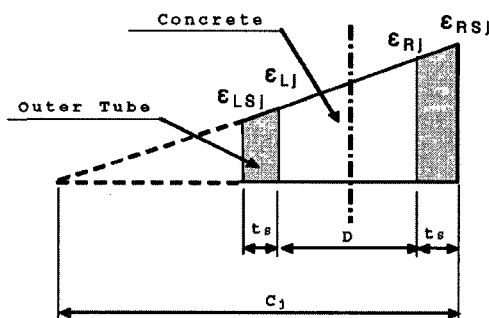


Fig. 4 Strain Distribution on a CFT Column

Fig. 3 shows a cross section of a CFT column. The diameter of the confined concrete is denoted as D and the thickness of the outer tube is denoted as t_s . If the center of the column section is set as the (0,0) point of the x-y coordinate system, the outline and the inner line of the internal tube can be defined as the functions of x , $y_s(x)$ and $y_{cc}(x)$, respectively. These functions are given by Eq. 1 and Eq. 2.

$$y_s(x) = \sqrt{\left(\frac{D+2t_s}{2}\right)^2 - x^2} \quad (\text{Eq. 1})$$

$$y_{cc}(x) = \sqrt{\left(\frac{D}{2}\right)^2 - x^2} \quad (\text{Eq. 2})$$

where, D : diameter of the confined concrete , t_s : thickness of the outer tube

The same stages of strain distribution used for prior columns are applied to this derivation. For a particular stage of strain distribution, axial forces and moments on the longitudinal reinforcements are calculated as follows. The confined concrete is divided into small particles as shown in Fig. 3 and the area of the i th particle of the confined concrete, A_{CCi} , is given by Eq. 3. The x coordinate of the i th particle of the confined concrete is denoted as x_{CCi} .

$$A_{CCi} = 2 \int_{x_{CCi}}^{x_{CCi+1}} y_{cc}(x) dx \quad (\text{Eq. 3})$$

$$\Delta x_{CC} = \frac{D}{N_{CC}} \quad , \quad x_{CCi} = i \Delta x_{CC} - \frac{D}{2} \quad (\text{Eq. 4})$$

where, N_{CC} : number of divided confined concrete particles
 Δx_{CC} : length of divided confined concrete particle
 x_{CCi} : x coordinate of the i th particle of confined concrete
 A_{CCi} : area of the i th particle of the confined concrete

The strain at the i th particle is given as Eq. 6 and the corresponding stress on the i th particle is computed from the developed concrete model. The axial force and the moment on the confined concrete at the j th stage of the strain distribution are given as Eq. 6 and Eq. 7.

$$\epsilon_{CCi,j} = \epsilon_{Lj} + i \Delta \epsilon_j \Delta x_{CC} \quad (\text{Eq. 5})$$

$$P_{CCj} = \sum_{i=0}^{N_{CC}} A_{CCi} \frac{f_{CC}(\epsilon_{CCi,j}) + f_{CC}(\epsilon_{CCi+1,j})}{2} \quad (\text{Eq. 6})$$

$$M_{CCj} = \sum_{i=0}^{N_{CC}} P_{CCi} \frac{x_{CCi} + x_{CCi+1}}{2} \quad (\text{Eq. 7})$$

where, $\epsilon_{CCi,j}$: strain on the i th particle of the confined concrete at the j th stage of the strain distribution

If the outer tube is divided into small particles as shown in Fig. 4, the area of the i th particle of the outer tube, $A_{S i}$, is given by Eq. 8 and Eq. 9. The x coordinate of the i th particle of the outer tube is denoted as $x_{S i}$.

$$A_{S i} = 2 \int_{x_{S i}}^{x_{S i+1}} y_s(x) dx \quad : \quad \text{when } x^2 > \left(\frac{D+2t_s}{2}\right)^2 \quad (\text{Eq. 8})$$

$$A_{S i} = 2 \int_{x_{S i}}^{x_{S i+1}} y_s(x) - y_{cc}(x) dx \quad : \quad \text{when } x^2 \leq \left(\frac{D+2t_s}{2}\right)^2 \quad (\text{Eq. 9})$$

$$\Delta x_S = \frac{D+2t_s}{N_S} \quad (\text{Eq. 10})$$

$$x_{S i} = i \Delta x_S - \frac{D+2t_s}{2} \quad (\text{Eq. 11})$$

- where, N_S : number of divided outer tube particles
 Δx_S : length of divided outer tube particles along x-axis
 $x_{S i}$: x coordinate of the i th particle of outer tube
 $A_{S i}$: area of the i th particle of outer tube

The strain distribution on the column section is shown in Fig. 4 at the j th stage. The strains at the left and right far end of the outer tube, $\epsilon_{LS j}$ and $\epsilon_{RS j}$, are given by Eq. 12 and Eq. 13 respectively. The strain at the i th particle of the internal tube is given by Eq. 115 at the j th stage of the strain distribution

$$\epsilon_{LS j} = \frac{D-c_j-t_s}{D-c_j} \epsilon_{L j} = \frac{c_j-D-t_s}{c_j} \epsilon_{R j} \quad (\text{Eq. 12})$$

$$\epsilon_{RS j} = \frac{c_j+t_s}{c_j} \epsilon_{R j} \quad (\text{Eq. 13})$$

$$c_j = D \frac{\epsilon_{R j}}{\epsilon_{R j} - \epsilon_{L j}} \quad (\text{Eq. 14})$$

$$\epsilon_{S i,j} = \epsilon_{LS j} + i \Delta \epsilon_j \Delta x_S \quad (\text{Eq. 15})$$

The stress on the i th particle is computed from the corresponding material model for the given strain. The axial force and the moment on the internal tube at the j th stage of the strain distribution are given as Eq. 16 and Eq. 17.

$$P_{S j} = \sum_{i=0}^{N_S} A_{S i} \frac{f_S(\epsilon_{S i,j}) + f_S(\epsilon_{S i+1,j})}{2} \quad (\text{Eq. 16})$$

$$M_{Sj} = \sum_{i=0}^{N_s} P_{Si} \frac{x_{Si} + x_{S_{i+1}}}{2} \tag{Eq. 17}$$

where, $\epsilon_{S_{i,j}}$: strain on the i th particle of the outer tube at the j th stage of the strain distribution

Thus for the j th stage of the strain distribution, the total axial force and the total moment acting on the entire column section are given by Eq. 18 and Eq. 19 respectively. The interaction diagram is obtained by plotting the point of (M_j, P_j) at every stage of the strain distribution.

$$P_j = P_{CCj} + P_{Sj} \tag{Eq. 18}$$

$$M_j = M_{CCj} + M_{Sj} \tag{Eq. 19}$$

3. Numerical Examples and Verifications

With derived equations in prior section, a computer program is coded. This program have two analysis options which consider the confining effect of the concrete and the strain hardening of the steel or not. Fig. 5 shows the difference of the interaction diagrams when the confining effect and strain hardening are considered or not. And also the results from present developed model are compared with the results from AIJ specification and Kato's research (1995) in Fig. 6.

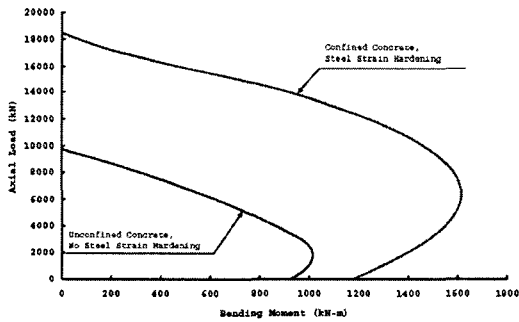


Fig. 5 P-M Interaction Diagrams of a CFT Column

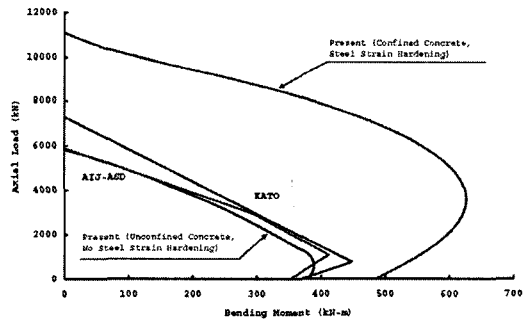


Fig. 6 Comparison of Interaction Diagrams with AIJ and Kato

Table 1 Geometric and Material Properties

Diameter of the Confined Concrete	55.88cm
Thickness of the Outer Tube	10mm
Compressive Strength of Unconfined Concrete	21.7MPa
Yield Strength of the Outer Tube	250MPa
Ultimate Strength of the Outer Tube	392.4MPa
Modulus of Elasticity of the Outer Tube	206010MPa
Ultimate Strain of the Outer Tube	0.160

Table 2 Geometric and Material Properties

Diameter of the Confined Concrete	33.848cm
Thickness of the Outer Tube	9mm
Compressive Strength of Unconfined Concrete	29.43MPa
Yield Strength of the Outer Tube	323.73MPa
Ultimate Strength of the Outer Tube	480.69MPa
Modulus of Elasticity of the Outer Tube	206010MPa
Ultimate Strain of the Outer Tube	0.20

Because the current specifications and Kato's research don't consider the increased strength of confined concrete, their results are similar to the resent result when the confining effect is not considered. But considering the confining effect, the results are significantly different. The geometric and material properties of the column in Fig. 5 are summarized in Table 1. And the geometric and material properties of the column in Fig. 6 are summarized in Table 2.

Fig. 7 shows the verification of the present interaction model for a CFT column. The small circles are experimental results by Fam (2004). The results from present model considering the confining effect accords with the experimental results. On the other hand results from specifications such as AISC, CAN/CSA and AIJ are significantly different from the experimental results because these specifications cannot consider the enlarged strength of the confined concrete. Thus the present interaction model is a realistic and accurate model.

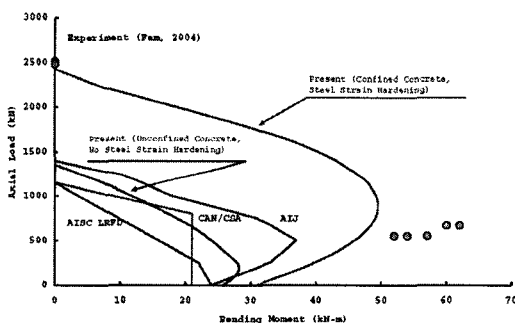


Fig. 7 Verification of Present Interaction Model for a CFT Column

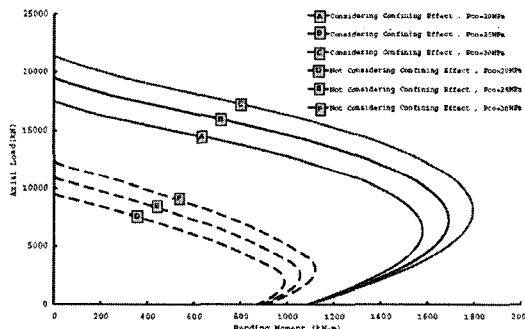


Fig. 8 Interaction Diagrams of CFT Columns by the Change of Concrete Strength

The information of the CFT specifications tested by Fam (2004) are as follows. The steel tubes used for the construction of the CFT specifications were cold formed and welded steel tubing. The outside diameter of the tubes D_o was 152.4mm and the thickness of the wall was 3.12mm. The diameter and wall thickness of the tube resulted in a (D_o / t_s) ratio of 49. This ratio satisfies the limitations specified by different specifications, including the American AISC LRFD (1998), the Canadian CAN/CSA-S16. 1-94 (1994), and the Japanese AIJ (Qie 1994). The yield strengths of the steel tube were 347 and 382 MPa in tension and compression respectively from test. The moduli of elasticity were 189 and 198 GPa in tension and compression, respectively. The ultimate elongation in tension was 29% and the average Poisson's ratio was 0.25. Ready-mixed concrete was used to fill the steel tubes. A total of twenty standard size cylinders were cast and cured under the same conditions as the CFT columns. Based on the cylinder test results at the time of testing, the concrete compressive strengths were 55 MPa. The tensile strength and Poisson's ratio were 4.7 MPa and 0.2, respectively. Fig. 8 show interaction diagrams of CFT columns which have different concrete strength. Lines A, B, and C are the

interaction diagram considering the confining effect and the strain hardening when the strengths of unconfined concrete are 20 MPa, 25 MPa, and 30 MPa, respectively. And lines C, D, and E are the interaction diagram when the confining effect and the strain hardening are not considered. The geometric and material properties of the column in Fig. 42 are summarized in Table 3.

Table 3 Geometric and Material Properties

Diameter of the Confined Concrete	60cm
Thickness of the Outer Tube	8mm
Compressive Strength of Unconfined Concrete	20, 25, 30MPa
Yield Strength of the Outer Tube	250MPa
Ultimate Strength of the Outer Tube	392.4MPa
Modulus of Elasticity of the Outer Tube	206010MPa
Ultimate Strain of the Outer Tube	0.16

4. Conclusion

A nonlinear CFT column model was developed considering the confining effect on the concrete in a CFT column in this study. This developed model was verified by experimental results from other researchers and compared with the results of various specifications. From the comparison of experimental results (Fam, 2004), current specifications are too conservative and not accurate to design a reasonable CFT column. Thus it is necessary to introduce the concept of confining effect on concrete for reasonable and economic CFT columns. The developed nonlinear column model in this study can help to design and analyze a reasonable and economic CFT column.

감사의 글

본 연구는 한국건설기술평가원에서 시행한 『2005년도 건설핵심기술연구개발사업 (과제번호: D02-01)』의 연구비 지원과 『삼성물산(주) 건설부문』의 부분 지원에 의하여 수행되었으며, 지원기관에 깊은 감사를 표합니다.

참고문헌

- 황원섭, 김동조, 정대안 (2003) 콘크리트 구속효과를 고려한 CFT단주의 극한강도, 대한토목학회논문집, 제 23권, pp.1011-1018
- AASHTO LRFD (1998) Bridge Design Specifications.
- ACI Committee 318 (1999) Building Code Requirements for Structural Concrete (318-99) and Commentary (318R-99), *American Concrete Institute*
- Amir Fam, Frank S. Qie, Sami Rizkalla (2004) Concrete-Filled Steel Tubes Subjected to Axial Compression and Lateral Cyclic Loads, *Journal of Structural Engineering*, ASCE, Apr., pp.631-640
- M. J. N. Priestley and R. Park (1987) Strength and Ductility of Concrete Bridge Columns under Seismic Loading, *ACI Structural Journal*, Title no. 84-s8, 61-76